Supplemental Material

Journal of Climate

Pattern Recognition Methods to Separate Forced Responses from Internal Variability in Climate Model Ensembles and Observations

https://doi.org/10.1175/JCLI-D-19-0855.1

Supporting Information for "Pattern Recognition Methods to Separate Forced Responses from Internal Variability in Climate Model Ensembles and Observations"

Robert C. J. Wills[1], David S. Battisti[1], Kyle C. Armour[1], Tapio Schneider[2], Clara Deser[3]

[1]University of Washington, Seattle, WA
[2]California Institute of Technology, Pasadena, California
[3]National Center for Atmospheric Research, Boulder, Colorado

Linear Inverse Model Optimal Perturbation Filter

Here we describe the linear inverse model (LIM) optimal perturbation filter (LIMopt), which was identified by F17 as one of the best available method for estimating the forced climate response from a single ensemble member. We then compare it to the LFP filtering method presented in the main text.

LIMs assume that the evolution of anomalies $\mathbf{x}$ (e.g., SST anomalies) are described by a multivariate linear Markov process (i.e., a first-order Ornstein-Uhlenbeck process)

$$\frac{d\mathbf{x}}{dt} = \mathbf{L}\mathbf{x} + \xi, \tag{1}$$

where $\mathbf{L}$ is a linear operator and ξ is white noise (e.g., Penland and Sardeshmukh 1995). The best estimate of the state vector $\mathbf{x}(t)$, is given by forward integration according to $\mathbf{x}(t+\tau) = \mathbf{G}(\tau)\mathbf{x}(t)$, where $\mathbf{G}(\tau) = \exp(\mathbf{L}\tau)$. The evolution of the state vector can be decomposed into a sum of nonnormal eigenmodes

$$\mathbf{x}(t) = \textstyle\sum_i \mathbf{u}_i \alpha_i(t), \tag{2}$$

where $\mathbf{u}_i$ are the eigenvectors of $\mathbf{L}$, estimated from the ensemble-mean covariance matrix $\langle \mathbf{C} \rangle$ and the ensemble-mean lag-1 covariance matrix $\langle \mathbf{C}_1 \rangle$ by

$$\mathbf{L} = \frac{1}{\tau} \ln \left[\langle \mathbf{C}_1 \rangle \langle \mathbf{C} \rangle^{-1} \right]. \tag{3}$$

Here, we have allowed for the use of multiple ensemble members, but this holds also for the case of a single ensemble member. The time evolution $\alpha_i(t)$ is determined from the projection of $\mathbf{x}$ onto the corresponding adjoint eigenvector. The eigenmodes are either stationary damped modes with a single spatial pattern and decay time or a damped oscillatory mode with two patterns. The first eigenmode is the one with the least damping, and will generally capture any long-term forced response in the dataset (Compo and Sardeshmukh 2010; Newman 2013; F17). This framework is generally applied to seasonal SST anomalies, with $\tau = 3$ months; we will apply it here to seasonal surface temperature anomalies (including land and sea ice). The dimensionality is reduced by working in a truncated EOF space, in our case with 50 EOFs to account for around 77% of the total variance.

Corresponding author: Robert C. Jnglin Wills, `rcwills@uw.edu`

Following F17, we employ a LIM-based optimal perturbation filter (LIMopt) to identify a spatiotemporally varying estimate of the forced response in CESM-LE surface temperatures. This method was used by Solomon and Newman (2012) to isolate (and remove) ENSO variability within Pacific SSTs and by F17 to isolate the forced response within global SSTs. The optimal initial structure $\Phi_1(\tau_e)$ is the pattern that evolves into the maximum possible anomaly after time τ_e, taken here to be 2.5 yr (as in F17, but much longer than the 6-9 months used by Solomon and Newman (2012) to isolate the ENSO signal). It is the normalized right singular eigenvector of $\mathbf{G}(\tau_e) = \exp(\mathbf{L}\tau_e)$. The LIMopt filter considers the evolution of anomalies from this optimal initial structure over a longer time period τ_1. The forced response is given by

$$\mathbf{F} = \sum\nolimits_{\tau=0}^{\tau_1} \alpha(t-\tau)\mathbf{G}(\tau)\Phi_1(\tau_e), \tag{4}$$

where $\alpha(t)$ is determined by projection of the left singular vector $\Psi_1(\tau_e)$ onto the anomaly at that point in the iteration, i.e.,

$$\alpha(t) = \left[\mathbf{x}(t) - \sum\nolimits_{\tau=0}^{\tau_1} \alpha(t-\tau)\mathbf{G}(\tau)\Phi_1(\tau_e)\right]\Psi_1(\tau_e), \tag{5}$$

with the initial condition $\alpha(0) = \mathbf{x}(0)\Psi_1(\tau_e)$. This method considers all anomalies that evolve from the optimal initial structure, which allows the spatial pattern to evolve over time.

In order to apply LIMopt to multiple ensemble members, in addition to averaging over multiple ensemble members in the computation of $\langle\mathbf{C}\rangle$ and $\langle\mathbf{C}_1\rangle$, one must replace $\mathbf{x}(t)$ with $\langle\mathbf{x}(t)\rangle$ in Eq. 5. Alternatively, one could use the opposite order of operations where the iterative procedure (Eqs. 4 and 5) is applied to each ensemble member separately and then the resulting forced response estimate $\mathbf{F}$ is averaged over the ensemble. However, this arrives at the same answer after a longer computation time.

We apply LIMopt to the CESM-LE seasonal surface temperature anomalies. We use $\tau_e = 2.5$ yr (as in F17), but try two different choices of τ_1: $\tau_1 = 20$ yr (as in F17) and $\tau_1 = 0$ (which uses the optimal perturbation pattern, but skips the iterative filtering). The results are compared to LFP filtering in Fig. S1. While LIMopt provides a much better estimate of the forced response than the unfiltered data (i.e., a simple ensemble mean), it generally does not perform as well as LFP filtering. In particular, it does not improve the forced response estimate as much with the addition of ensemble members. Focusing on the case of a single ensemble member, LFP filtering achieves a better correlation with the forced response of grid-point temperatures (Fig. S1a), global-mean surface temperature (Fig. S1c), North Atlantic SST (Fig. S1d), and US surface temperature (Fig. S1f), but LIMopt achieves a marginally better correlation with the forced response of the Pacific east-west SST difference (Fig. S1e). In terms of global-mean RMSE, they perform about the same (Fig. S1b).

Also of note is that LIMopt with $\tau_1 = 0$ generally performs similar to or slightly better than LIMopt with $\tau_1 = 20$ yr, indicating that the iterative filtering procedure does not substantially improve the forced response estimate. Simply identifying the optimal perturbation pattern is the main benefit derived from the LIMopt analysis. A potential explanation for this is that the LIMopt filter (with $\tau_1 > 0$) uses the LIM to smooth over unforced variations, but in doing so can introduce anomalies that are not actually present in the data set. So while this filtering improves the estimate of the forced response in a single ensemble member (Fig. S1, cf. F17), it can introduce small errors at the local scale, which prevent it from generalizing well to larger ensemble sizes (Fig. S1).

Here we analyzed which method works best for isolating the forced response from a single ensemble member. While LIMopt may perform better for the pattern of tropical SST change (Fig. S1e), LFP filtering performs better on average (Fig. S1a), including for global-mean surface temperature (Fig. S1c). Comparing with the work of F17,

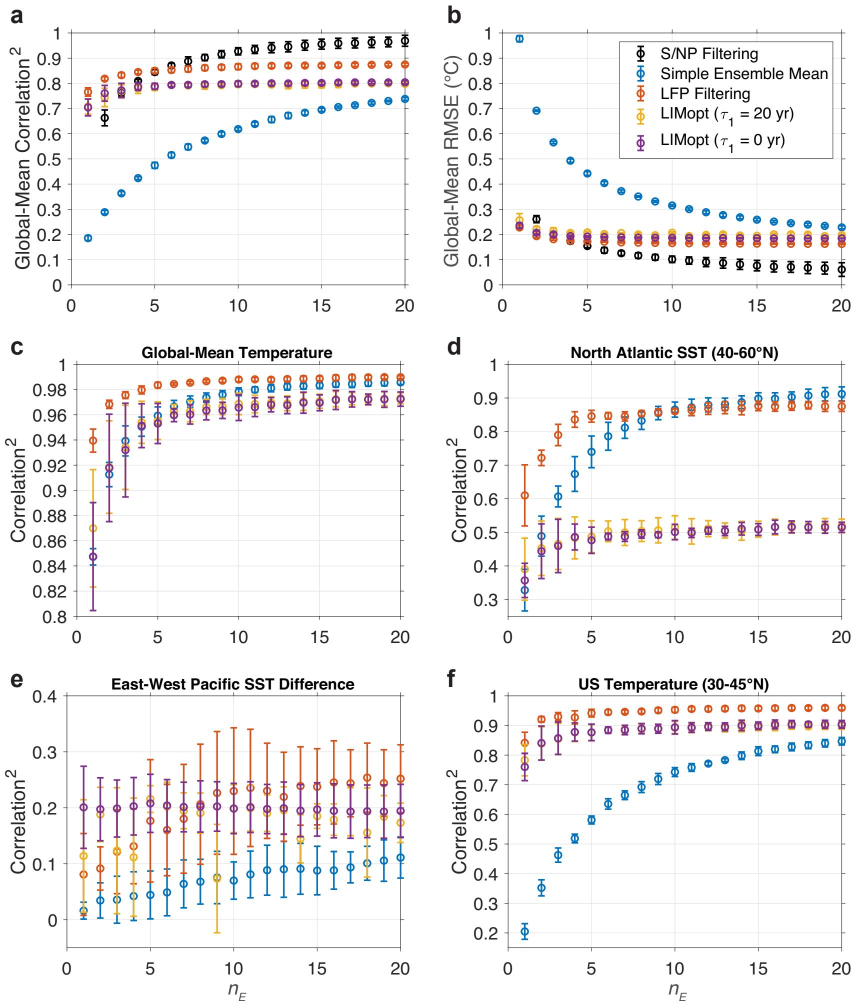

Figure S1. As in Fig. 1, except with the addition of LIMopt forced response estimates. For legibility, S/NP filtering is omitted from panels (c)-(f).

this also means that LFP filtering performs better than a linear trend, quadratic trend, regression against global-mean SST, or multi-variate ensemble empirical mode decomposition. Additionally, its similarity to S/NP filtering makes it easily generalizable to different ensemble sizes. Moreover, LFP filtering is a purely statistical method and makes no assumptions about the nature of the underlying dynamics, as LIM-based methods do. Overall this make LFP filtering the best available method for isolating forced responses in small ensembles or single realizations.

References

Compo, G. P., & Sardeshmukh, P. D. (2010). Removing ENSO-related variations from the climate record. *J. Climate*, *23*(8), 1957–1978.

Newman, M. (2013). An empirical benchmark for decadal forecasts of global surface temperature anomalies. *J. Climate*, *26*(14), 5260–5269.

Penland, C., & Sardeshmukh, P. D. (1995). The optimal growth of tropical sea surface temperature anomalies. *J. Climate*, *8*(8), 1999–2024.

Solomon, A., & Newman, M. (2012). Reconciling disparate twentieth-century Indo-

Pacific ocean temperature trends in the instrumental record. *Nature Climate Change*, *2*(9), 691.